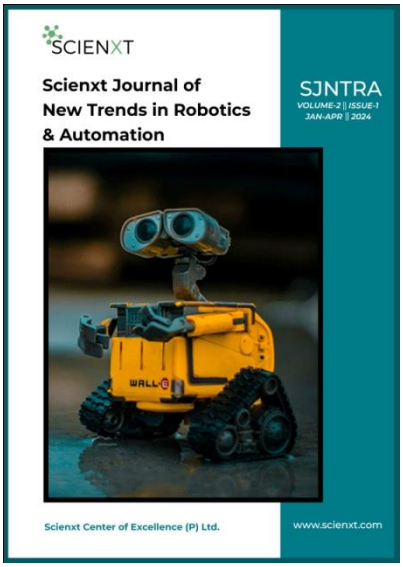

Scienxt Journal of New Trends In Robotics & Automation
Volume-2 || Issue-1 || Jan-Apr || Year-2024 || pp. 1-17

Review of a framework for simulation of magnetic soft robots using the material point method

[1]Mr. Suraj K.R, [2]Dr. Mallikarjun P. Y
[1]Student, Department of ECE, DSATM, Bengaluru
[2]Professor & HOD, Department of ECE, DSATM, Bengaluru

**Corresponding Author: Mr. Suraj K.R*
Email: surajkhimavat236h@gmail.com

Abstract:

This abstract presents a framework for simulating Magnetic Soft Robots (MSRs) using the Material Point Method (MPM). The framework integrates hyper-elastic material models with the magnetic wrench induced under external fields, allowing for the accurate representation of MSR behavior. In contrast to Finite Element Methods (FEM), the MPM framework inherently models self-collision and captures the effect of forces in non-homogeneous magnetic fields. The document demonstrates the MPM framework's ability to model the influence of magnetic wrenches on MSRs, capture dynamic behavior under time-varying magnetic fields, and provide an accurate representation of deformation when colliding with obstacles. Additionally, the framework is validated through comparisons with real-world MSR designs from the literature, showcasing its capability to replicate complex behaviors seen in real robots in simulation.

Keyword:

Taichi**,** Magnetic beam Deformation, Finite Element Method (FEM).

1. Introduction:

The field of robotics is constantly evolving, with engineers pushing the boundaries of what's possible. Magnetic soft robots (MSRs) represent a fascinating new chapter in this story. MSRs have attracted considerable interest due to their potential for miniaturization enabled by off-board actuation . Unlike traditional robots reliant on motors and gears, MSRs leverage the power of magnetism for movement. This unique approach unlocks exciting possibilities, particularly for tasks requiring handiness and miniaturization.

MSRs are essentially tiny robots crafted from soft, elastic materials – think stretchy polymers – embedded with magnetic particles . These magnetic inclusions are the key to their operation. By strategically manipulating an external magnetic field, we [30] can exert a force and torque (known as a wrench) on the MSR. This allows for precise control over the robot's movement and orientation, making it ideal for navigating intricate environments.

Imagine a scenario where traditional robots struggle – exploring confined spaces within delicate machinery or maneuvering through the complex internal structures of a building. MSRs, with their inherent flexibility and wireless control via magnetic fields, could excel in such situations. Their soft bodies allow them to navigate tight corners and delicate surfaces without causing damage.

However, simulating the behavior of MSRs presents a significant challenge. Traditional modeling techniques often rely on dividing the robot's body into a mesh of elements. This approach, known as the Finite Element Method (FEM), becomes computationally expensive and less accurate for robots that undergo large deformations [10], [11], a hallmark of MSRs. To simplify FEM modeling, the assumption of discrete hard magnetic elements embedded within the soft material is often made. However, this assumption loses accuracy as deformation increases. Zhao et al. addressed this by deriving a stress relationship for magnetically hard, mechanically soft materials and integrating it into FEM software (ABAQUS), enabling continuous, deformable magnetic profiles within the material [11]. Despite its accuracy, nonlinear FEM analysis incurs significant computational costs, and mesh distortion under large deformation can lead to erroneous results and poor convergence [15].

This is where the Material Point Method (MPM) can step in as a potential game-changer [16], [17]. The MPM is a hybrid Lagrangian-Eulerian model for continuum mechanics, offering advantages over Finite Element Methods (FEM) by providing a cyclical process that moves between a particle-based representation and a fixed grid. This approach allows for the accurate representation of the deformation experienced in magnetic soft materials, particularly

under high deformation and in the presence of non-homogeneous magnetic fields. This method offers several advantages:

- Enhanced Accuracy: MPM can more accurately capture the large deformations experienced by MSRs during movement.
- Reduced Computational Cost: By avoiding the mesh generation step, MPM can potentially be more computationally efficient.
- Self-Collision Handling: MPM inherently accounts for self-collision – instances where different parts of the MSR come into contact with each other during movementeliminating the need for additional calculations.

In this work, we extend MPM to model magnetically hard and mechanically soft materials, demonstrating its capability to model large MSR deformations under varying fields. Our system can represent dynamic behavior, collisions, and equilibrium states in static fields. Additionally, each particle in the MPM representation is associated with its magnetization vector, enabling the modeling of varied and near-continuous magnetization profiles. We [30] showcase the ability to model torques and magnetic forces present in non-homogeneous magnetic fields, with implicit self-collision handling allowing the study of physical interactions between robot segments. External forces can be easily integrated into the model, providing realistic interactions with surfaces and obstacles. Validation of the models on real-world MSR designs from the literature showcases the framework's capability to replicate complex behaviors seen in real robots in simulation.

2. Methodology:

2.1. The material point method:

(MPM) stands as a pivotal numerical technique in continuum mechanics, integrating elements from both Eulerian and Lagrangian frameworks. It operates through two fundamental material representations: the Lagrangian perspective, comprising discrete particles of fixed mass and volume that effectively discretize the material, and the Eulerian viewpoint, which employs an undeformable grid fixed within a reference frame. In this grid, nodes are evenly spaced and remain static, facilitating the transfer of properties between different time steps.

Within MPM, the exchange of information between these representations occurs via two key processes: Particle-to-Grid (P2G) and Grid-to-Particle (G2P). During P2G, properties from the particles are transferred to the grid nodes, while G2P involves the

$$W(\Delta r) = w(\Delta x)w(\Delta y)w(\Delta z) \quad (1)$$

where

Where $\Delta r = [\Delta x, \Delta y, \Delta z]^T$ is the relative displacement between the particle and the node at i, j, k a. $\alpha \in \{\Delta x, \Delta y, \Delta z\}$. As such grid mass is distributed as with each other during movement eliminating the need for additional calculations.

In this work, we [30] extend MPM to model magnetically hard and mechanically soft materials, demonstrating its capability to model large MSR deformations under varying fields. Our system can represent dynamic behavior, collisions, and equilibrium states in static fields. Additionally, each particle in the MPM representation is associated with its magnetization vector, enabling the modeling of varied and near-continuous magnetization profiles. We [30] showcase the ability to model torques and magnetic forces present in non-homogeneous magnetic fields, with implicit self-collision handling allowing the study of physical interactions between robot segments. External forces can be easily integrated into the model, providing realistic interactions with surfaces and obstacles. Validation of the models on real-world MSR designs from the literature showcases the framework's capability to replicate complex behaviors seen in real robots in simulation. interpolation of properties from the grid back to the particles.

2.2. Particle (lagrangian) representation:

Particles are initialized to represent the geometry of the soft robot and their position at time t is notated as xt p ∈ R3. vt p ∈ R3 represents the particle velocity vector and Ct p ∈ R3×3 represents the affine velocity matrix . A final variable Ft p ∈ R3×3 represents the particle deformation gradient initialized to the identity matrix F0 p = I.

2.3. Particle to grid (P2G):

To transfer the particle representation of the material to the grid, we [30] must distribute the properties of the particle to the surrounding nodes. Here, the properties are distributed using a quadratic B-spline kernel distributed to a 3 × 3 × 3 neighborhood of grid nodes given as

$$w(\alpha) = \begin{cases} 0.75 - |\alpha/\delta x|^2 & 0 \le |\alpha/\delta x| < 0.5 \\ 0.5(1.5 - |\alpha/\delta x|)^2 & 0.5 \le |\alpha/\delta x| < 1.5 \\ 0 & 1.5 \le |\alpha/\delta x| \end{cases} \quad (2)$$

$M^t_{i,j,k} = \Sigma p\ W(\Delta r) mp,$ (3)

where m_p is the particle mass equal to ρv_p where ρ is the material density and v_p is the particle particle volume. Grid momentum is calculated as

$p^t_{i,j,k} = \Sigma_p\ W(\Delta r)\ (\ m_p v^t_p - (\ 4\ /\delta x 2 v_p p^t_p p (F^t_p)^T + m_p C_n{}^p\ )\ \Delta r\ )$ (4)

where $P^t{}_p$ is the first Piola–Kirchhoff stress tensor

2.4. Grid (eulerian) representation:

After transfer to the grid representation, the effect of external forces is imposed (Fig. 1(c)). These external forces and the grid momentum can be integrated to form the grid velocity.

$$V^t_{i,j,k} = 1 / m^t_{i,j,k}(p^t_{i,j,k} + f^t_{i,j,k}\Delta t), \quad (5)$$

where Δt is the simulation time stepping and $f^t_{i,j,k}$ is the external force on the node. For all nodes where $m^t_{i,j,k} \neq 0$.

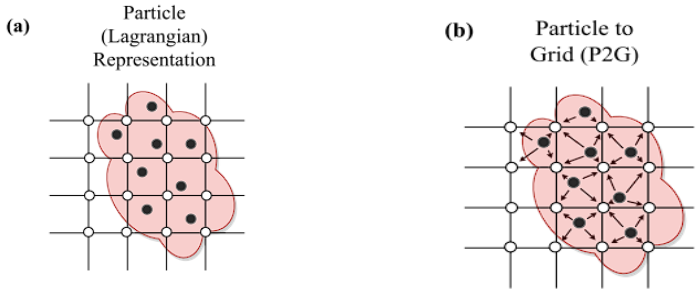

Figure. 1 : (a) Internal forces and magnetic stress are computed in the particle domain. (b) Particle properties are transferred to grid representation. (c) External interaction and forces due to magnetic gradients are computed in the grid domain. (d) Particle properties are reconstructed from the grid

Our research endeavors to extend the Moving Least Squares - Material Point Method (MLS-MPM) algorithm to accurately model the actuation experienced within magnetic materials. MLS-MPM incorporates the Moving Least Squares (MLS) interpolation technique into MPM, offering a smoother representation of particle properties. For a comprehensive exploration of MLS-MPM, readers are encouraged to delve into the detailed discussions provided by [18] and [19].

mixed, this composite material is poured into molds corresponding to the desired shape of the magnetic robot and allowed to set [23]. Subsequently, the cast undergoes exposure to a saturating magnetizing field to establish the desired direction of magnetization. Upon removal from the magnetic field, the material retains a remnant magnetization.

2.5. Grid to particle (G2P):

After the velocities in the grid frame have been calculated, particle velocity and affine velocity can then be reconstructed utilizing the same weighting kernel specified in Section II-B (Fig. 1(d)).

$$V^{t+1}{}_p = \Sigma\Sigma\Sigma\ W(\Delta r)v^t_{i,j,k}, \quad (6)$$

$$C^{t+1}{}_p = \frac{4}{\delta x^2} \Sigma_i \Sigma j \Sigma_k \, W(\Delta r) v^t{}_{i,j,k} \Delta r. \quad (7)$$

The deformation gradient of the particle and particle positions are updated, representing the overall change in deformation and pose of material in the time step.

$$F^{t+1}{}_p = (\| + C_p{}^{t+1} \Delta t) \, F^t{}_p \quad (8)$$

$$X^{t+1}{}_p = x^t{}_p + v^{t+1}{}_p \Delta t \quad (9)$$

External interaction and forces due to magnetic gradients are computed in the grid domain. (d)particles properties are reco

3. Modeling techniques:

In the realm of soft robotics, a common approach involves the utilization of elastomers embedded with magnetic elements. Typically, this entails mixing a silicone prepolymer with hard magnetic microparticles, often NdFeB owing to its notable remnant magnetization. Once mixed, this composite material is poured into molds corresponding to the desired shape of the magnetic robot and allowed to set [23]. Subsequently, the cast

undergoes exposure to a saturating magnetizing field to establish the desired direction of magnetization. Upon removal from the magnetic field, the material retains a remnant magnetization.

In our research, we [30] regard this material as an ideal hard-magnetic soft material . Notably, we neglect the self-interaction among the magnetic elements within the Magnetic Soft Robot (MSR). This simplification has proven valid in modeling MSR deformation, as the relative strength of this self-interaction pales in comparison to the interaction with larger external magnetic fields .

3.1. Elastomeric properties:

For modeling the elastic properties of the material the NeoHookean elastic model is adopted which has been shown to accurately model the stress-strain relationship of magnetic soft

materials in the strain ranges experienced in soft robotic applications . The Neo-Hookean model is given as

$$P^t_{p\ elastic} = GJ^{-2/3}\left(F^t_p - \frac{I^1}{3} F^{-T}\right) + KJ(J-1)F^{-2} . \quad (10)$$

Where $P^t_{p\ elastic}$ is the elastic contribution of the first Piola-Kirchoff stress tensor, G is the shear modulus of the material and K is the bulk modulus. J = determinant(Ft p) and I1 = trace(FtT p Ft p). To satisfy the assumption of near incompressibility of the utilized silicone polymers we chose the bulk modulus to be a sufficiently high value. In this case, we set K = 20G. At the strain/scale ranges relevant to our MSRs, the actual value of the bulk modulus does not largely affect the final deformation .

3.2. Magnetic properties:

torque between the magnetic moment and the external field.

$$\tau = m \times B \quad (11)$$

where B is t$m^t_{i,j,k}$A magnetic agent under external magnetic fields will experience an aligning he external magnetic field and m is the magnetic moment vector. Further, in the case of a non-homogeneous magnetic field, the agent will experience a force,

$$f = \nabla(B \cdot m). \quad (12)$$

This force is proportional to the spatial gradient of the magnetic field and is at maximum with the alignment of the magnetic moment and external field. In the FEM approach outlined by Zhao et al. the effect of aligning torque under homogeneous magnetic fields is integrated into the elastic model via an additional stress. We [30]utilize this stress along with the Neo-Hookean model in the P2G step of the MPM cycle. This, in the first Piola-Kirchoff form, is

$$P^t_{p\ magnetic} = -1/\mu_0\ B \otimes B_{rp}, \quad (13)$$

where $\otimes$ is the dyadic product and Brp is the remnant magnetic flux density associated with the particle.

$$P^t_p = P^t_{p\ elastic} + P^t_{pmagnetic}. \quad (14)$$

By incorporating the magnetic stress effect into the P2G, step, the effect of the realigning torque can be incorporated into the MPM. However, the forces induced in non-homogeneous magnetic fields are not covered. Therefore the magnetic force is incorporated as an external force in the grid velocity calculation. To calculate the force at the grid node, we calculate the equivalent magnetic moment of the node as a product of the volume of magnetic particles using the same weightings as described in the P2G Section II-B

$$= v_p\mu_p/\mu_o \Sigma\ W(\Delta r)\tilde{B}_{rp}. \quad (15)$$

where $\tilde{B}_{rp}$ is the remnant magnetic flux density rotated into the current reference frame. The external magnetic force can then be derived as

$f_{magnetic} = \nabla B_{i,j,k}{}^{T} \cdot m^{t}_{i,j,k}$, (16)

where $\nabla B_{i,j,k}$ is the spatial gradient of the magnetic field at the node.

3.3. Material damping:

complex factors (viscosity, air resistance, temperature change, etc.). To capture these properties Deceleration is the rate at which an object transmits downward and represents several of magnetic soft materials, we model damping by adding a force proportional to the current lattice motion,

$f_{damping} = -cp^{t}_{i,j,k}$ (17)

where c is the damping constant. This external force will drive the object into the final equilibrium state creating a stable applied field. So there is a full range of external forces entering the network phase

$f^{t}_{i,j,k} = f_{magnetic} + f_{damping} + f_{gravity}$(18) $f^{t}_{i,j,k} = \nabla B_{i,j,k}{}^{T} \cdot m^{t}_{i,j,k} - c\mathbf{p}^{t}_{i,j,k} + m^{t}_{i,j,k}g$(19).

where g is the acceleration due to gravity. It should be noted that the proposed MPM extension for modeling magnetic soft materials requires three material parameters that are easily obtained. These are the material density, magnetic residue, and shear parameters of the material. However, being humble will be much harder. In magnetics, one is usually interested in the final equilibrium state of the robot, so the damping parameter that results in the fastest settling time of the system is most appropriate This can be achieved by repeated testing. In cases where accurate modeling of complexity is required, the approach followed by Shariat et al. can be used .

4. Experimental verification:

4.1. Implementation:

The Taichi programming language was used to develop the magnetic material point method (MPM) algorithm, which was simulated on an NVIDIA Quadro RTX 4000 GPU with selected GPU parallelization support and Python-like syntax

It is important to balance the velocity model and the stability in determining the time step for the simulation. As shown in , the maximum time step $(\Delta t_{max})$for the MPM is given by:

$$\Delta t_{max} = c\frac{\delta x}{\sqrt[3]{\rho}}\frac{1}{3G}$$

Here C is a constant close to one. Larger network node spacing can increase the time step but

sacrifice fidelity when external forces are added. The initial particle distribution is obtained by creating the same 3D model of the robot geometry.

After empirically validating the method on planar models to ensure consistency with real-world practice, a full 3D implementation of the magnetic MPM framework is presented, simulating magnetic soft robots (MSRs) from existing literature and material parameters obtained following the method shown in the center and by [24] .

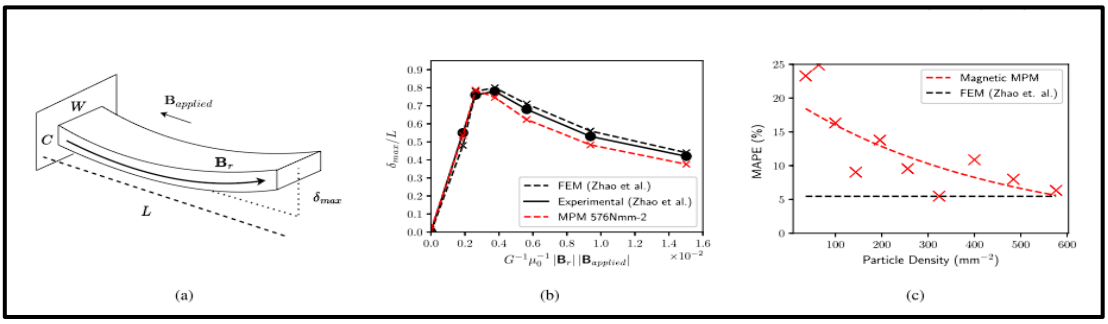

Figure. 2. High deformation magnetic soft beam experiment as presented by Zhao et al. [11]

(a) The applied field Bapplied is in the opposite direction to the remnant magnetization Br of the soft material leading to high deflection. (L = 17.2 mm, C = 0.84 mm, W = 5 mm). (b) Magnetic MPM methodology compared with experimental results and FEM analysis [11] G−1μ−1 0 |Br| is a constant which leads these results to be independent of material parameters. (c) Mean Absolute Percentage Error (MAPE) converges with increased particle density.

4.2. Magnetic beam deformation:

To validate our method, we repeated [30] the beam-bending experiment of Zhao et al. [11]. We used a magnetically strong but mechanically soft beam made of PDMS (Sylgard 184) with parameters (G = 303 kPa) and (|Br| = 0.258 T), we made it a vector with an external magnetic field coherent with it in contrast to the residual the magnetization of the beam.

With increasing field strength, this pattern reversed (see Fig. 2(a)).We recreated this situation in our system by changing the size of the particles to match the beam (δx = 0.3 mm), (Δt = 6 *10-6 s). We contrasted the resulting deflection (δ_{max} /L) with the authors' experimental FEM data (Fig. 2 (b)).

The effects are consistent with the densities proven in Figure 2(c), in which the mean average error (MAPE) of 576 mm-2 particle size was determined to be 6.1% As a result of this take a look at Therefore, we're capable of select smaller complexes for similarly trying out. .

4.3. Deformation under non-homogeneous magnetic fields:

We [30] investigated the interaction between a magnetic soft robot (MSR) and a permanent magnet to evaluate the ability of the MPM system to generate forces from magnetic field gradients MSR of Ecoflex 30 silicon polymer blended with NdFeB microparticles (1:1). in) of a sample mass ratio), magnetized with its major axis 100 mm x 0 mm measurement placed on a circular neodymium magnet, with a residualcapacityof1.44T

In this configuration, no magnetic torque was observed due to the alignment of the magnetization of the robot with the permanent magnet. The MSR structure showed periodic changes in thickness to induce more distortion compared to the plain beam, where the stronger parts increased the total magnetic moment and the stronger parts of flat surfaces experienced larger strains due to lower elastic forces the MSR magnet using linear steps can transport, to extend the length of the large magnetic field gradient encountered

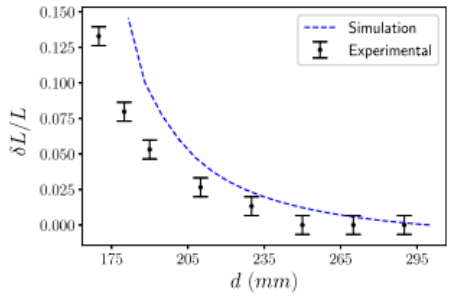

Figure. 3: Comparison of simulation and experimental results for the deformation of the robot as described in Section IV-C due to increasing field gradient forces as it's introduced towards the magnet

Simulation parameters included (δx = 2 mm, Δt = 1 × 10−6 s, N = 15,359) particles. Comparative analysis of strain between simulation and experimental setup (as shown in Fig. 3) revealed strong agreement. While some error at lower distances to the magnet was noted, it was attributed to limitations inmagnetic field modeling and hyper-elastic model accuracy, rather than a flaw in the methodology.

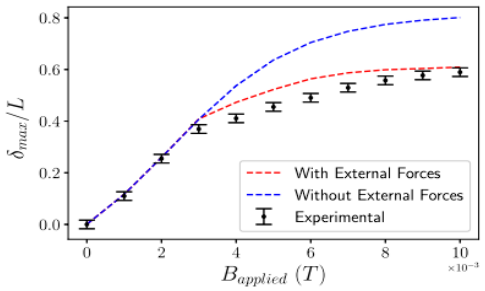

Figure. 4: Comparison of maximum normalized deflection δmax/L of the MSR with experimental results when external interaction is considered. (δx = 2 mm, Δt = 5 × 10−5 s, N = 11,520)

4.4. Interaction with external bodies:

Automatic material point interfaces in the material point method (MPM) are treated implicitly, providing some significant advantages over finite element method (FEM) methods

that require additional mesh design between vertices to handle such collisions External forces can be incorporated into the internal model without the complexity of the mesh representation.

To demonstrate the capability of the MPM system to model interactions with external objects, we [30] investigated the deformation of an axially magnetically magnetic soft robot (MSR) in contact with a rigid obstacle.

$$v_{out}=\begin{cases}0 & if\ v_{in}\geq 0\\ v_{in} & otherwise\end{cases}$$

where v_{in} represents the input velocity and $v_{out}$is the velocity used in particle mode reconstruction.

The MSR with dimensions of 60 × 3 × 3 mm consists of Dragonskin-10 silicone polymer doped with NdFeB microparticles at 1:1 mass ratio Simulation results (depicted in Fig. 4) Considering that an external component has an MPM framework in which the normalized maximum deflection of the applied magnetic field is $\frac{\delta}{L}_{\max}$show It should be noted that, at large deflections, a noticeable difference in tip position is observed, which may be due to the accuracy limit of the underlying hyperelastic model at high deformations

4.5. Magnetic soft robots from the literature:

In this section, we update the magnetic soft robot (MSR) system from the literature to show the adaptability of our MPM system:

1) Developmental MSR (Pittiglio et al.,): We adopted their methodology. In a range of magnetic and non-magnetic materials, we have . An optimization technique was used to estimate each block's magnetization vector so that, in a given magnetic field, the desired shape could be obtained. Our method's efficiency was validated by the simulation findings, which were more consistent and resembled real-world behavior under the same magnetic field (see Fig. 5(a)).

2) Small soft robots (Hu et al.): We emulate horizontal interactions by using the collision model, as per Hu et al. . We did this again while using a rotating external magnetic field with different strengths (refer to Fig. 5(b)). The authors' observation of "walking" behavior shows our system's capacity to carry out several intricate tasks.

3) Unclamped six-arm receiver (Xu et al., 2013): We adhere to Xu et al., 2013, and demonstrate the impact-based trapping behavior.Simulation results(See Fig. 5(c)). demonstrated the robot's ability to fold up and grasp small objects upon the application of a perpendicular magnetic field, These examples highlight the potential of the MPM framework for iterative design and testing of MSRs, offering advantages over complex fabrication and experimental setups. Additionally, the inherent ability of MPM to handle self-collision simplifies the modeling process compared to FEM approaches.

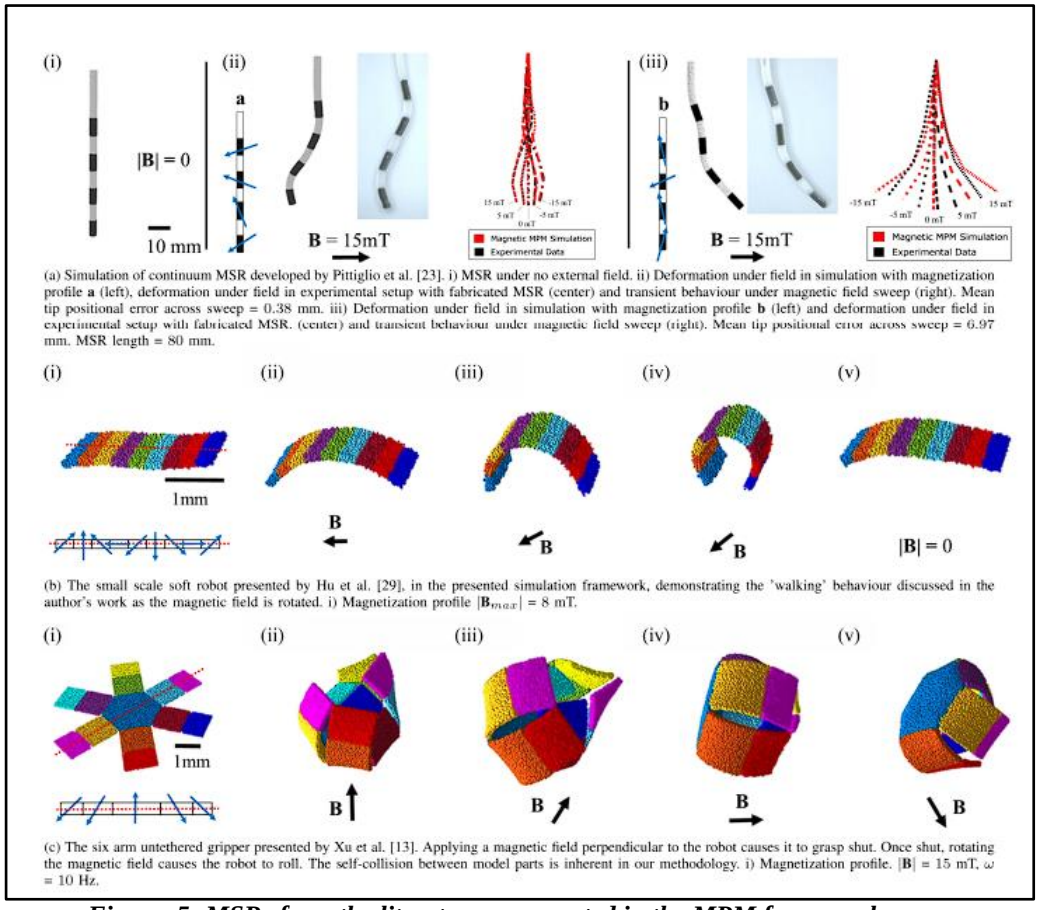

Figure. 5: MSRs from the literature represented in the MPM framework

5. Conclusion:

We [30] have introduced a fresh approach to MSR simulation in this paper. The deformation encountered can be correctly represented by the Material Point Method (MPM). In the presence of external magnetic fields in magnetic soft materials at extreme deformation. In contrast to FEM techniques, MPM allows MSRs that depend on self-interaction to be represented because it implicitly depicts self-collisions in the material. Furthermore, by the integration of the magnetic forces encountered in non-homogeneous magnetic fields, our methodology has expanded the capabilities of already available systems. The methodology

has been tested, and the results demonstrate a significant agreement with real-world deformation at large strains (6.1% MAPE, Fig. (c)). Additionally, a comparison with MSRs from the literature demonstrates how well the suggested methodology may replicate the complicated behavior observed in real robots. For MSR simulation, existing frameworks have frequently depended on unpublished, closed-source, or proprietary implementations.

We have made our magnetic MPM framework implementation examples available so that others can make use of our approach. 3D computer-aided design (CAD) models that specify the magnetic profile of every piece can be used to create robots. When compared to fabrication and experimental setups, the speed at which concepts may be tested via simulation enables the rapid iterative design of MSRs. Complex behaviors may be evaluated and ideas can be examined and adjusted when combined with the capacity to model outside influences and impediments. We anticipate that by making our implementation publicly available, other people working on simulation frameworks will be able to directly compare our work with theirs. Our framework is ideal for training or optimizing machine learning systems that may be implemented in real-world scenarios. For instance, simpler rigid-link models were used to optimize Pittiglio et al.'s continuum MSRs . These designs could be closer to the intended goal or include dynamic behavior under the impact of transient magnetic fields if more precise modeling was used. Our implementation's mass parallelization uses GPU processing to produce efficient runtimes.

The MPM is a continuous function of the starting variable values, in contrast to FEM. Hu et al. took advantage of this fact .to create a completely differentiable physics simulation to cut down on the number of design optimization iterations required for convergence.

This may be repeated using our methods to effectively optimize parameters including robot shape, applied field, and magnetic profile.

The methodology that is being given solely takes into account the interplay between the actuating field applied externally and the material's magnetic field. Any self-interaction between the discrete magnetic robot segments is ignored in this. This assumption works well for the examples in our experimental verification, but it might not accurately describe the behavior of alternative MSR designs that depend on this interaction. The forces that interplay when several MSRs are present in the same workspace could serve as an illustration of this . Future research could take into account the field created by distinct magnetic segments to more accurately depict this property. Naturally, this would make the simulation much more complex in terms of algorithms and processing. One potential application of MPM's intrinsic particle collision representation capability is to examine the interplay between MSRs and

external soft bodies. Because of the therapeutic uses of MSRs to investigate the relationship between robots and soft tissues, this is especially interesting.

6. Reference:

(1) Y. Kim and X. Zhao, "Magnetic soft materials and robots," Chem. Rev., vol. 122, no. 5, pp. 5317–5364, 2022.

(2) M. Sitti, "Miniature soft robots–road to the clinic," Nature Rev. Mater., vol. 3, no. 6, pp. 74–75, 2018.

(3) D. Liu et al., "Magnetically driven soft continuum microrobot for intravascular operations in microscale," Cyborg Bionic Syst., vol. 2022, 2022.

(4) J. Lu, Y. Liu, W. Huang, K. Bi, Y. Zhu, and Q. Fan, "Robust control strategy of gradient magnetic drive for microrobots based on extended state observer," Cyborg Bionic Syst., vol. 2022, 2022.

(5) C. Huang, Z. Lai, X. Wu, and T. Xu, "Multimodal locomotion and cargo transportation of magnetically actuated quadruped soft microrobots," Cyborg Bionic Syst., vol. 2022, 2022, Art. no. 0004.

(6) E. Diller and M. Sitti, "Micro-scale mobile robotics," Found. Trends Robot., vol. 2, no. 3, pp. 143–259, 2013.

(7) Q. Boehler, S. Gervasoni, S. L. Charreyron, C. Chautems, and B. J. Nelson, "On the workspace of electromagnetic navigation systems," IEEE Trans. Robot., vol. 39, no. 1, pp. 791–807, Feb. 2022.

(8) Y. Kim, G. A. Parada, S. Liu, and X. Zhao, "Ferromagnetic soft continuum robots," Sci. Robot., vol. 4, no. 33, 2019, Art. no. eaax7329.

(9) P. Lloyd, G. Pittiglio, J. H. Chandler, and P. Valdastri, "Optimal design of soft continuum magnetic robots under follow-the-leader shape forming actuation," in Proc. Int. Symp. Med. Robot., 2020, pp. 111–117.

(10) H. Ye, Y. Li, and T. Zhang, "Magttice: A lattice model for hard-magnetic soft materials," Soft Matter, vol. 17, no. 13, pp. 3560–3568, 2021.

(11) R. Zhao, Y. Kim, S. A. Chester, P. Sharma, and X. Zhao, "Mechanics of hard-magnetic soft materials," J. Mechanics Phys. Solids, vol. 124, pp. 244–263, 2019.

(12) R. Dreyfus, Q. Boehler, and B. J. Nelson, "A simulation framework for magnetic continuum robots," IEEE Robot. Automat. Lett., vol. 7, no. 3, pp. 8370–8376, Jul. 2022.

(13) T. Xu, J. Zhang, M. Salehizadeh, O. Onaizah, and E. Diller, "Millimeterscale flexible robots with programmable three-dimensional magnetization and motions," Sci. Robot., vol. 4, no. 29, 2019, Art. no. eaav4494.

(14) S. Jeon et al., "A magnetically controlled soft microrobot steering a guidewire in a three-dimensional phantom vascular network," Soft Robot., vol. 6, no. 1, pp. 54–68, 2019.

(15) J. Danczyk and K. Suresh, "Finite element analysis over tangled simplicial meshes: Theory and implementation," Finite Elements Anal. Des., vol. 70–71, pp. 57–67, 2013.

(16) W. T. Solowski, "Material point method: Overview and challenges ahead," in Advances in Applied Mechanics, vol. 54, S. P. Bordas and D. S. Balint, Eds., Amsterdam, The Netherlands: Elsevier, 2021, ch. 2, pp. 113–204.

(17) Y. Hu et al., "Chainqueen: A real-time differentiable physical simulator for soft robotics," 2018. [Online]. Available: https://arxiv.org/abs/1810.01054

(18) F. Sun, G. Wang, L. Zhang, R. Wang, T. Cao, and X. Ouyang, "Material point method for the propagation of multiple branched cracks based on classical fracture mechanics," Comput. Methods Appl. Mechanics Eng., vol. 386, 2021, Art. no. 114116.

(19) M. Li, Y. Lei, D. Gao, Y. Hu, and X. Zhang, "A novel material point method (MPM) based needle-tissue interaction model," Comput. Methods Biomech. Biomed. Eng., vol. 24, no. 12, pp. 1393–1407, 2021.

(20) Y. Hu et al., "A moving least squares material point method with displacement discontinuity and two-way rigid body coupling," ACM Trans. Graph., vol. 37, no. 4, 2018, Art. no. 150.

(21) C. Jiang, C. Schroeder, A. Selle, J. Teran, and A. Stomakhin, "The affine particle-in-cell method," ACM Trans. Graph., vol. 34, no. 4, pp. 1–10, 2015. SIGGRAPH 2016 Courses. New York, NY, USA: ACM, 2016, doi: 10.1145/2897826

(22) C. Jiang, C. Schroeder, J. Teran, A. Stomakhin, and A. Selle, "The.2927348. C. Jiang, C. Schroeder, A. Selle, J. Teran, and A. Stomakhin, "The affine particle-in-cell method," ACM Trans. Graph., vol. 34, no. 4, pp. 1–10, 2015.

(23) G. Pittiglio et al., "Patient-specific magnetic catheters for atraumatic autonomous endoscopy," Soft Robot., vol. 9, pp. 1120–1133, 2022.

(24) T. Da Veiga et al., "Material characterization for magnetic soft robots," in Proc. IEEE 4th Int. Conf. Soft Robot., 2021, pp. 335–342.

(25) A. Shariati, J. Shi, S. Spurgeon, and H. A. Wurdemann, “Dynamic modeling and visco-elastic parameter identification of a fiber-reinforced soft fluidic elastomer manipulator,” in Proc. IEEE/RSJ Int. Conf. Intell. Robots Syst., 2021, pp. 661–667.

(26) Y. Hu, T.-M. Li, L. Anderson, J. Ragan-Kelley, and F. Durand, “Taichi: A language for high-performance computation on spatially sparse data structures,” vol. 38, no. 6, pp. 1–16, 2019, doi: 10.1145/3355089.3356506.

(27) Y. Fang, Y. Hu, S.-M. Hu, and C. Jiang, “A temporally adaptive material point method with regional time stepping,”Comput. Graph. Forum, vol. 37, no. 8, pp. 195–204, 2018.

(28) M. Ortner and L. G. Coliado Bandeira, “Magpylib: A free Python package for magnetic field computation,” SoftwareX, vol. 11, 2020, Art. no. 100466.

(29) W. Hu, G. Z. Lum, M. Mastrangeli, and M. Sitti, “Small-scale soft-bodied robot with multimodal locomotion,” Nature, vol. 554, no. 7690, pp. 81–85, 2018.

(30) Joshua Davy, Peter Lloyd, James H. Chandler, “A Framework for Simulation of Magnetic Soft Robots Using the Material Point Method”,2023.